In-plane shear properties of medium-density fibreboard measured by asymmetric four-point bending of a notched specimen

Hiroshi Yoshihara, Shungo Suzuki and Masahiro Yoshinobu

Faculty of Science and Engineering, Shimane University, Nishikawazu-cho 1060, Matsue, Shimane 690-8504, Japan

Corresponding author: Hiroshi Yoshihara
E-mail: yosihara@riko.shimane-u.ac.jp
Telephone: +81-852-32-6508
Fax: +81-852-32-6123

Abstract In this research, asymmetric four-point bending (AFPB) tests were used to obtain the in-plane shear (IPS) properties of medium-density fibreboard (MDF). Circular notches were cut on the top and bottom surfaces of rectangular MDF bars with variable distances between the notch roots. Both tab-free and tabbed specimens were prepared from these bars. The AFPB tests were conducted using these specimens, and three IPS properties, that is, the shear modulus, proportional limit stress, and stress at failure, were measured. When using tabs, the IPS properties could be obtained for a wide range of the notch root distances, although the failure initiated at the notch roots led to the catastrophic failure.

Introduction

Medium-density fibreboard (MDF) is one of the principal wood products used in various construction projects. To ensure that construction designs are reliable and cost-effective, it is important to accurately measure the in-plane shear (IPS) properties of MDF, including the in-plane shear modulus (IPSM), the in-plane shear stress at the proportional limit (IPSPL), and the in-plane shear strength (IPSS).

The asymmetric four-point bending (AFPB) test is one effective method to determine the shear properties of a material. Several examples describing the examination of the shear properties for ceramic and textile composites (Ünal et al. 1998; Ünal and Dayal 2003; Tarnopol'skii et al. 1999, 2000), solid wood (Yoshihara and Suzuki 2005; Morita et al. 2006; Yoshihara 2009), laminated veneer lumber (LVL) (Ohno et al. 2010), plywood (Yoshihara 2010~~a~~; Yoshihara and Yoshinobu 2014), and paper (Yoshihara and Yoshinobu 2015a) are included.

Due to the fabrication process, the density of the MDF in the region close to the mid-thickness is usually lower than that at the surface (Schulte and Frühwald 1996, De Magistris and Salmén 2004; Wilczyński and Kociszewski 2007; Sliseris et al. 2014; Sebera et al. 2014). Therefore, it is relatively easy to induce interlaminar shear failure around the mid-thickness region. Several examples describing the measurement of the out-of-plane shear (OPS) properties using a simple shear test (Schulte and Frühwald 1996; Suzuki and Miyagawa 2003) and using a short beam shear test (Suzuki et al. 1987; Yoshihara 2012~~a~~,

2013) have been reported. For the IPS properties, there are several available examples that can be employed when determining the IPSM using vibration tests (Yoshihara 2011; Yoshihara and Yoshinobu 2015b) and plate bending test based on full-field slope measurements (Xavier et al. 2013). In contrast, it is difficult to induce shearing force failure in MDF, and there are few examples available that describe measuring the IPSS, with the exception of those relating to the rail shear test (McNatt 1969; Lee and Stephens 1988; Suzuki et al. 2000; Suzuki and Miyagawa 2003). The rail shear test is determined in several major standards (ASTM 1037-12, BS EN789-2004). However, when using the rail shear method, there are concerns that the failure will be always induced at the gripped portion where a combined stress condition is inevitable, and that is why we are trying to use AFPB test method to see if it will work better. Additionally, this method requires a special equipment for applying the shearing force, which extremely restricts the specimen configuration.

As described, it is important to evaluate the IPS properties of MDF used in construction projects, making it is necessary to establish a method for accurately characterising the IPS properties. AFPB test may be promising to achieve this aim because the IPS properties of solid wood can be obtained accurately without using any special equipment (Yoshihara 2009). In this study, the shear properties of MDF were therefore measured by AFPB tests using a beam specimen with circular notches. The specific objectives in this study are summarised as:

1. Examination of the validity of AFPB test.
2. Investigation on the effect of end tabs used for preventing the specimen from the

bending failure at the loading points.

3. Investigation on the effect of distance between the circular holes.

Materials and methods

Specimens

Medium-density fibreboard (MDF) with dimensions of 910 mm × 1820 mm × 15 mm was used to fabricate the test specimens for this study. The board, with a density of 609 ± 9 kg m^{-3} and a moisture content (MC) of 12 % was fabricated in a board mill (Ueno Mokuzai Kogyo Co., Himeji, Japan) using softwood with a typical fibre length of 2-4 mm and urea-formaldehyde (UF) resin. The material was stored for approximately one year at a constant 20°C and 65% relative humidity prior to testing. The material was confirmed to be in an air-dried condition. These conditions were maintained throughout the testing. The equilibrium MC condition was approximately 12%.

Similarly to the definitions utilised in previous studies (Nairn 2009; Matsumoto and Nairn 2009), the directions along the length, width, and thickness of the MDF sheet are defined as the L, T, and Z directions, respectively.

Independently of the AFPB test, the Young's modulus and IPSM were measured by flexural vibration tests using the specimen cut from the MDF. In the vibration tests, a beam specimen with the dimensions of 260 (L) × 40 (T) × 15 (Z) was prepared. Similar to the

method conducted in a previous study (Yoshihara 2011), flexural vibration tests were conducted using five specimens. From the vibration tests, the details of which are described in Yoshihara (2011), the Young's modulus in the L direction E_L and IPSM G_{LT} were obtained as 3.545 ± 0.240 and 0.980 ± 0.075 GPa, respectively.

Asymmetric four-point bending (AFPB) test

Initially, rectangular bars with the dimensions of 260 mm × 40 mm were cut from the MDF raw material. The length and depth directions of the specimen coincided with the L and T directions of the MDF sheet, respectively. As shown in Figure 1, both tab-free and tabbed specimens were prepared. In the tabbed specimen, four rectangular tabs of Japanese birch with a thickness of 10 mm were bonded on both ends of the specimen using epoxy resin as shown in Figure 1(b). It was expected that bending failure at the loading or supporting point could be reduced using the tabs. For both specimens, two 4-mm-diameter circular holes were drilled symmetrically on the mid-span point on the LT plane. Straight notches with a width of 3 mm were then cut using a circular saw. The distance between the notch roots H was varied from 5 to 30 mm at intervals of 5 mm. A triaxial strain gauge (Tokyo Sokki FRA-2-11, gauge length = 2 mm, base length = 8 mm) was bonded at a centre of the LT plane to measure the IPS strain γ_{LT}, with the exception of the specimen with H = 5 mm, in which a triaxial strain gauge with the gauge length of 1 mm (Tokyo Sokki FRA-1-11, base length = 4 mm) was used. In a previous study on the AFPB test of solid wood and acryl, the stress

concentration was effectively reduced and the stress distribution was almost uniform (Yoshihara 2009). Therefore, it was expected that the he stress concentration could be effectively reduced in this study. For the tab-free AFPB test specimen, failure at the point behind the inner loading or supporting point was most common. Therefore, it was expected that bending failures would be reduced by increasing the specimen width at the loading and supporting points. Therefore, the specimens containing solid wood tabs bonded using an epoxy resin were also prepared.

The specimens were asymmetrically supported and loaded, as shown in Figure 1(a). Before loading, the specimens were set so that the notches were at the mid-span. The total span length was 240 mm, and the specimens were eccentrically supported at two trisected points. The load *P* was applied to the remaining two trisected points using a crosshead speed of 2 mm/min until the load markedly decreased. Figure 2 shows the set-up of the AFPB test. The total testing time was approximately 5 min. The IPS stress τ_{LT} was calculated from the following equation based on beam theory (Yoshihara 2009):

$$t_{LT} = \frac{P}{2HB}, \tag{1}$$

where *B* is the width of the specimen, which coincides with the thickness of the MDF sheet (= 15 mm). The IPS strain γ_{LT} was obtained from the strain-gauge output (Yoshihara 2009):

$$g_{LT} = 2e_{45} - e_L - e_T, \tag{2}$$

where ε_L and ε_T are the normal strains in the L and T directions, respectively, and ε_{45} is the normal strain in the direction inclined at 45° with respect to the L direction. The in-plane shear modulus (IPSM) G_{LT} was measured from the initial inclination of the linear portion of

the τ_{LT}-γ_{LT} relationship. The IPS stress at the proportional limit (IPSPL) Y_{LT} was obtained from the stress at the onset of nonlinearity of the τ_{LT}-γ_{LT} relationship. There are several methods to determine the proportional limit stress (Davies et al. 2001). In this study, the proportional limit stress was determined from the stress where the half-thickness of the plotter trace deviated from the straight line drawn in the elastic region ($\tau_{LT} = G_{LT}\gamma_{LT}$) of the τ_{LT}-γ_{LT} relationship (Davies et al. 2001; Yoshihara 2014). The IPS stress at the occurrence of failure (IPSF) F_{LT} was derived from the maximum stress. In addition to the τ_{LT}-γ_{LT} relationship, the principal strain angle (PSA) ϕ during loading was obtained from (Yoshihara 2009):

$$\phi = \frac{1}{2}\tan^{-1}\left(\frac{\gamma_{LT}}{\varepsilon_T - \varepsilon_L}\right). \quad (3)$$

When $\phi = 45°$, the stress and strain fields are regarded as being in pure shear.

Two-dimensional finite element analyses (2D FEAs)

To analyze the stress distribution in the AFPB test, two dimensional finite element analyses (2D FEAs) were conducted independently of the AFPB tests. Finite element program was ANSYS Version 16.0, which is a library program of the Institute for Information Management and Communication of Kyoto University. Figure 3 shows the finite element model. The models had the dimensions of 260 mm (x = L), 40 mm (y = T), and 15 mm (z = Z) except for the notched region. The models consisted of four-noded plane-strain elements,

and the meshes were refined at the vicinity of the notches as demonstrated in Figures 3(b) and (c).

The Young's moduli in the L and T directions, E_L and E_T, respectively, and the shear modulus G_{LT} were determined by the flexural vibration tests as described above. The Poisson's ratio ν_{LT} was referred from a previous study (Yoshihara 2011). The values of E_L, E_T, G_{LT}, and ν_{LT} are: $E_L = E_T = 3.55$ GPa, $G_{LT} = 0.98$ GPa, and $\nu_{LT} = 0.275$.

The model was asymmetrically supported and loaded at the points (Figure 3(a)). The displacement of 1 mm was applied to inner and outer loading points. Similar to the actual AFPB tests, the details of which are described below, the distance between the notch roots, defined as *H*, was varied from 5 to 30 mm at intervals of 5 mm.

The shear stress distribution between the notch roots at the mid-length of the model and the reaction force at two loading points were calculated and compared with each other. The total of the reaction forces was substituted into *P* of Eq. (1), and the IPS value obtained from the reaction forces is defined as τ_{LT}^{BT}. In contrast, the shear stress corresponding to each node located between the notch roots at the mid-length is defined as τ_{LT}^{FEM}. The distance from the center of the model in the *y*-direction is defined as *y*, so the locations of the top and bottom hole edges correspond to $y = -0.5H$ and $0.5H$, respectively.

Results and discussion

2D FEAs

Figure 4(a) shows the $\tau_{LT}^{BT}/\ \tau_{LT}^{FEM}$-$y/H$ relationship between the hole edges corresponding to each H. The τ_{LT}^{FEM} value deviates from the τ_{LT}^{BT} value at the region near the hole edge. Figure 4(b) shows the $\tau_{LT}^{BT}/\ \tau_{LT}^{FEM}$-$y$ relationships in the range of -1 mm $\leq y \leq$ 1 mm, which corresponds to the gauge region except for the model with H = 5 mm. This figure indicates the shear stress is uniformly distributed in the gauge region, although the shear stress distribution is disturbed at the region close to the hole edge.

AFPB test

Figure 5 shows photographs of the failed AFPB test specimens. For the tab-free specimen, failure caused by the bending moment is easily induced at the point behind the inner loading or supporting point when the value of H is greater than 15 mm. Under these conditions, it was difficult to induce a failure in the gauge portion. In contrast, failure was initiated at the notch root and propagated within the gauge portion when the value of H is 5 or 10 mm. When bonding the tabs, the range of H values that induced failure at the notch root was extended to 5-20 mm. According to beam theory, the bending moment is usually reduced within the gauge portion during the AFPB test, meaning that a failure at the gauge portion may be regarded as being induced by a shearing force. In the solid wood AFPB test, catastrophic failure caused by shearing was induced along the fibre within the mid-depth of the gauge portion after the failure initiated at the notch root (Yoshihara ~~2012~~2009). However, as shown

in Figure 5, catastrophic failure was not induced at the mid-depth of the gauge portion, but rather was induced at the notch root due to the associated stress concentration.

Figure 6 shows typical examples of the IPS stress-strain (τ_{LT}-γ_{LT}) and PSA-IPS strain (ϕ-γ_{LT}) relationships. As shown in Figure 4(a), when the value of H is small enough, the τ_{LT}-γ_{LT} relationship continuously increases until a catastrophic failure was induced at the notch root. However, when examining the ϕ-γ_{LT} relationship, the value of ϕ tends to deviate from 45° before the IPS stress attained its maximum. It is possible that a small failure may have been induced at the notch root before attaining the maximum stress, which would cause a stress redistribution within the gauge portion (Yoshihara ~~2012~~2009). In contrast, as shown in Figure 4(b), failure by the bending moment preceded the shearing force induced failure when the value of H is large. Therefore, the stress at failure was lower than that of the specimen when the failure occurred in the notch root. In this failure pattern, the value of ϕ is approximately 45° until catastrophic bending failure was induced at the point behind the inner loading or the supporting point.

Figure 7 shows the IPSM G_{LT}, IPSPL Y_{LT}, and IPSF F_{LT} values corresponding to the distance between the notch roots H. Table 1 shows the results of analysis of variance (ANOVA) to compare and evaluate the differences between the average properties of G_{LT}, Y_{LT}, and F_{LT}. The results of ANOVA indicate that the difference between the G_{LT} values corresponding to each H value was not significant at a significance level of 0.05 for both the tab-free and tabbed specimens. In addition, the G_{LT} values obtained from the AFPB tests were close to 0.980 GPa, which was obtained from the flexural vibration test as described

above, and the results of ANOVA also indicated that the difference between the G_{LT} values obtained from the AFPB and vibration tests was not significant at a significance level of 0.05 for both the tab-free and tabbed specimens. Therefore, the G_{LT} value was appropriately measured by the AFPB test using both kinds of specimens. In contrast, the Y_{LT} and F_{LT} values decreased with increasing values of H. For the tab-free specimens, the statistical analysis revealed that the difference between the Y_{LT} values corresponding to each H value were significant at a significance level of 0.05. This phenomenon was also applicable to the F_{LT} values. In the tab-free specimen, the failure from the bending moment induced at the loading or supporting point often preceded that from shearing force at the gauge region, so the Y_{LT} and F_{LT} values decreased with increasing values of H. However, for the tabbed specimens, the difference between the Y_{LT} values with the H values of 5-25 mm is not significant, whereas that between the F_{LT} values is not significant in the range of H value is 5-15 mm. From these results, the use of end tabs was effective and permitted the measurement of Y_{LT} and F_{LT} values in over a wide range of H values and prevented failure from the bending moment at the inner loading or supporting point.

From the experimental results, it was revealed that the IPSM of the MDF can be appropriately obtained using an AFPB test with and without the tabs. In contrast, the tabbed specimen was preferable to obtain the IPSPL and IPSF values. In particular, it was feasible that the IPSF value of the specimen that failed in the gauge portion may be regarded as the in-plane shear strength (IPSS). Nevertheless, the stress concentration at the notch root cannot be reduced, and the failure initiated at the notch root led to catastrophic failure. As described,

this tendency is different from that of solid wood, in which the catastrophic failure was not induced at the notch root, but rather, at the mid-depth (Yoshihara ~~2012~~2009). Further research should be conducted to evaluate the IPSS of MDF by comparing the experimental results obtained from the AFPB test and other data such as from torsion testing, in which catastrophic failure may be induced using a specimen that does not contain any notches (Yoshihara 2011). Additionally, further research is also required whether the failure is really induced from the predominant shearing force. Microscopic observation may reveal the source of the failure.

Conclusions

The IPS properties of MDF, including the IPSM, IPSPL, and IPSS, were measured by AFPB testing using a specimen with circular notches. During the testing, tab-free and tabbed specimens with various distances between the notch roots were used. The conclusions are summarized as follows:

1. The IPSM value can be obtained using the tab-free and tabbed specimens with any distances between the holes *H* investigated in this study.
2. The end tabs were effective for inducing the shear failure at the gauge region while preventing the specimen from the bending failure at the loading points.
3. The results demonstrated the feasibility to measure the IPSPL and IPSS values when using the tabbed specimen with the *H* values of 5-25 and 5-15 mm, respectively.

Nevertheless, failure initiated at the notch root due to the stress concentration and often led to catastrophic failure.

Acknowledgments: This work was supported in part by a Grant-in-Aid for Scientific Research (C) (No. 24580246) from the Japan Society for the Promotion of Science.

References

ASTM D 1037-12 (2012) Standard test methods for evaluating properties of wood-base fiber and particle panel materials. ASTM International, West Conshohocken, PA, USA

BS EN 789-2004 (2004) Test methods. Determination of mechanical properties of wood based panels. BSI, London, UK

Davies P, Blackman BRK, Brunner AJ (2011) Mode II delamination. Fracture Mechanics Testing Methods for Polymers Adhesive and Composites ESIS Publication 28. Moore DR, Pavan A, Williams JG, ed. Elsevier, Amsterdam, pp 307-333

De Magistris F, Salmén L (2004) Combined shear and compression analysis using the Iosipescu device: analytical and experimental studies of medium density fiberboard. Wood Sci Technol 37(6): 509-521

Lee AWC, Stephens CB (1988) Comparative shear strength of seven types of wood composite panels at high and medium relative humidity conditions. Forest Prod J 38(3): 49-52

Matsumoto N, Nairn JA (2009) The fracture toughness of medium density fiberboard (MDF) including the effects of fiber bridging and crack-plane interference. Eng Fract Mech 76(18): 2748-2757

McNatt JD (1969) Rail shear test for evaluating edgewise shear properties of wood-base panel products. Forest Prod. Lab. Report 117: 1-15

Morita H, Fujimoto Y, Komatsu K, Murase Y (2006) Development of a shear testing method for full-sized structural lumber. Mokuzai Gakkaishi 52(6): 376-382

Nairn JA (2009) Analytical and numerical modeling of R curves for cracks with bridging zones. Int J Fract 155(2): 167-181

Ohno H, Kameyama Y, Suzuki H, Yoshida K, Matsumoto K, Ishiguri F, Yokota S, Iizuka K Yoshizawa N (2010) Shearing strength performance in laminated lumber composed of several softwoods with the same modulus of elasticity. Mokuzai Gakkaishi 56(3): 182-188

Schulte M, Frühwald A (~~1999~~1996) Shear modulus, internal bond and density profile of medium density fibre board (MDF). Holz Roh- Werkst 54(1): 49-55

Sebera V, Tippner J, Šimek M, Šrajer J, Děcký D, Klímová H (2014) Poisson's ratio of the MDF in respect to vertical density profile. Eur J Wood Prod 72(3): 407-410

Sliseris J, Andrä H, Kabel M, Dix B, Plinke B, Wiriadi O, Frolovs G (2014) Numerical prediction of the stiffness and strength of medium density fiberboards. Mech Mater 79: 73-84

Suzuki S, Piao CX, Saito F (1987) A study evaluating the internal bond properties of MDF. Bull. Fac. Agr. Shizuoka Univ 37: 55-60

Suzuki S, Nawa D, Miyamoto K, Shibusawa T (2000) Shear through-thickness properties of wood-based panels determined by the two-rail shear and edgewise shear methods. J Soc Mater Sci Jpn 49(4): 395-400

Suzuki S, Miyagawa H (2003) Effect of element type on the internal bond quality of wood-based panels determined by three methods. J Wood Sci 49(6): 513-518

Tarnopol'skii YM, Arnautov AK, Kulakov VL (1999) Methods of determination of shear properties of textile composites. Composites A 30(7): 879-885

Tarnopol'skii YM, Kulakov VL, Arnautov AK (2000) Measurement of shear characteristics of textile composites. Comput. Struct. 76(1-3): 115-123

Ünal Ö, Barnard DJ, Anderson IE (1999) A shear test method to measure shear strength of metallic materials and solder joints using small specimens. Scr Mater 40(3): 271-276

Ünal Ö, Dayal V (2003) Interlaminar shear strength measurement of ceramic composites by asymmetric four point bend shear test. Mater Sci Eng A 340(1-2): 170-174

Wilczyński A, Kociszewski M (2007) Bending properties of particleboard and MDF layers. Holzforschung 61(6): 717-722

Xavier J, Belini U, Pierron F, Morais J, Lousada J, Tomazello M (2013) Characterisation of the bending stiffness components of MDF panels from full-field slope measurements. Wood Sci Technol, 47(2): 423-441

Yoshihara H, Suzuki A (2005) Shear stress/shear strain relation of wood obtained by asymmetric four-point bending test of side-tapered specimen. J Test Eval 33(1): 55-60

Yoshihara H (2009) Shear properties of wood measured by the asymmetric four-point bending test of notched specimen. Holzforschung 63(2): 211-216

Yoshihara H (2010~~a~~) Edgewise shear properties of 5-ply wood obtained from the asymmetric four-point bending and uniaxial-tension tests of notched specimen. J Soc Mater Sci Jpn, 59(4): 291-296

~~Yoshihara H (2010b) Mode II critical stress intensity factor of medium-density fibreboard measured by asymmetric four-point bending tests and analyses of kink crack formation. Holzforschung 8(2): 1771-1789~~

Yoshihara H (2011) Measurement of the Young's modulus and shear modulus of in-plane quasi-isotropic medium-density fiberboard by flexural vibration. BioResources 6(4): 4871-4885

Yoshihara H (2012~~a~~) Interlaminar shear strength of medium-density fiberboard obtained from asymmetrical four-point bending tests. Construct Build Mater 34(1): 11-15

~~Yoshihara H (2012b) Shear modulus and shear strength evaluation of solid wood by a modified ISO 15310 square-plate twist method. Drvna industrija 65(1): 51-55~~

Yoshihara H (2013) Interlaminar shear strength of medium-density fiberboard (MDF) measured by three-point short-beam shear test and comparison with that obtained by asymmetric four-point bending test. Trans Jpn Mech Soc A 79(1): 105-115

Yoshihara H (2014) Plasticity analysis of the strain in the tangential direction of solid wood subjected to compression load in the longitudinal direction. BioResources 9(1): 1097-1110

~~Yoshihara H, Ohsaki H, Kubojima Y, Ohta M (2001) Comparisons of shear stress/shear strain relations of wood obtained by Iosipescu and torsion tests. Wood Fiber Sci 33(2): 275-283~~

Yoshihara H, Yoshinobu M (2014) Interlaminar shear strength of plywood measured by three-point and asymmetric four-point short beam shear test. Mokuzai Kogyo 69(5): 204-207

Yoshihara H, Yoshinobu M (2015a) In-plane shear strength of paper obtained by asymmetric four-point bending test. Holzforschung 69(1): 41-52

Yoshihara H, Yoshinobu M (2015b). Measurement of the in-plane shear modulus of medium-density fibreboard by torsional and flexural vibration tests. Measurement 60: 33-38

Figure captions

Fig. 1 (a) Tab-free specimen and diagram of the asymmetric four-point loading and (b) tabbed specimen. Units: mm. L and T represent the length and width directions of the MDF sheet, respectively.

Fig. 2 Asymmetric four-point bending (AFPB) test setup.

Fig. 3 Finite element model for the AFPB test. (a) Overall mesh, (b) detail of zone A, and (c) detail of zone B. Unit = mm.

Fig. 4 Distributions of the $\tau_{LT}^{FEM}/\ \tau_{LT}^{BT}$ values between the notch roots (a) and around the gauge region (b) obtained from the 2D FEAs.

Fig. 5 Typical failure patterns corresponding to the distance between the notch roots *H*. Failure is indicated in the ellipsoid except for the tabbed specimen with H = 30 mm.

Fig. 6 Typical examples of the shear stress/shear strain relation and the principal strain angle/shear strain relation. (a): Tabbed specimen with H = 15 mm, failure by shearing force at the gauge portion and (b): Tabbed specimen with H = 30 mm, failure by bending moment at the point behind the inner loading point.

Fig. 7 Shear modulus G_{LT}, proportional limit stress Y_{LT}, and stress at the occurrence of failure F_{LT} corresponding to the distance between the notch roots *H*. Results are average ± SD.

Table 1 Results of ANOVA to compare and evaluate the differences between the average properties of G_{LT}, Y_{LT}, and F_{LT}.

	Tab-free specimen			Tabbed specimen		
H (mm)	G_{LT}	Y_{LT}	F_{LT}	G_{LT}	Y_{LT}	F_{LT}
5	A	A		A	A	A
10	A	A		A	A	A
15	A			A	AB	AB
20	A	B		A	AB	B
25	A	BC		A	AB	
30	A	C		A	B	

Groups with same letters in column indicate that there is no statistical difference (significance level < 0.05) between the samples.

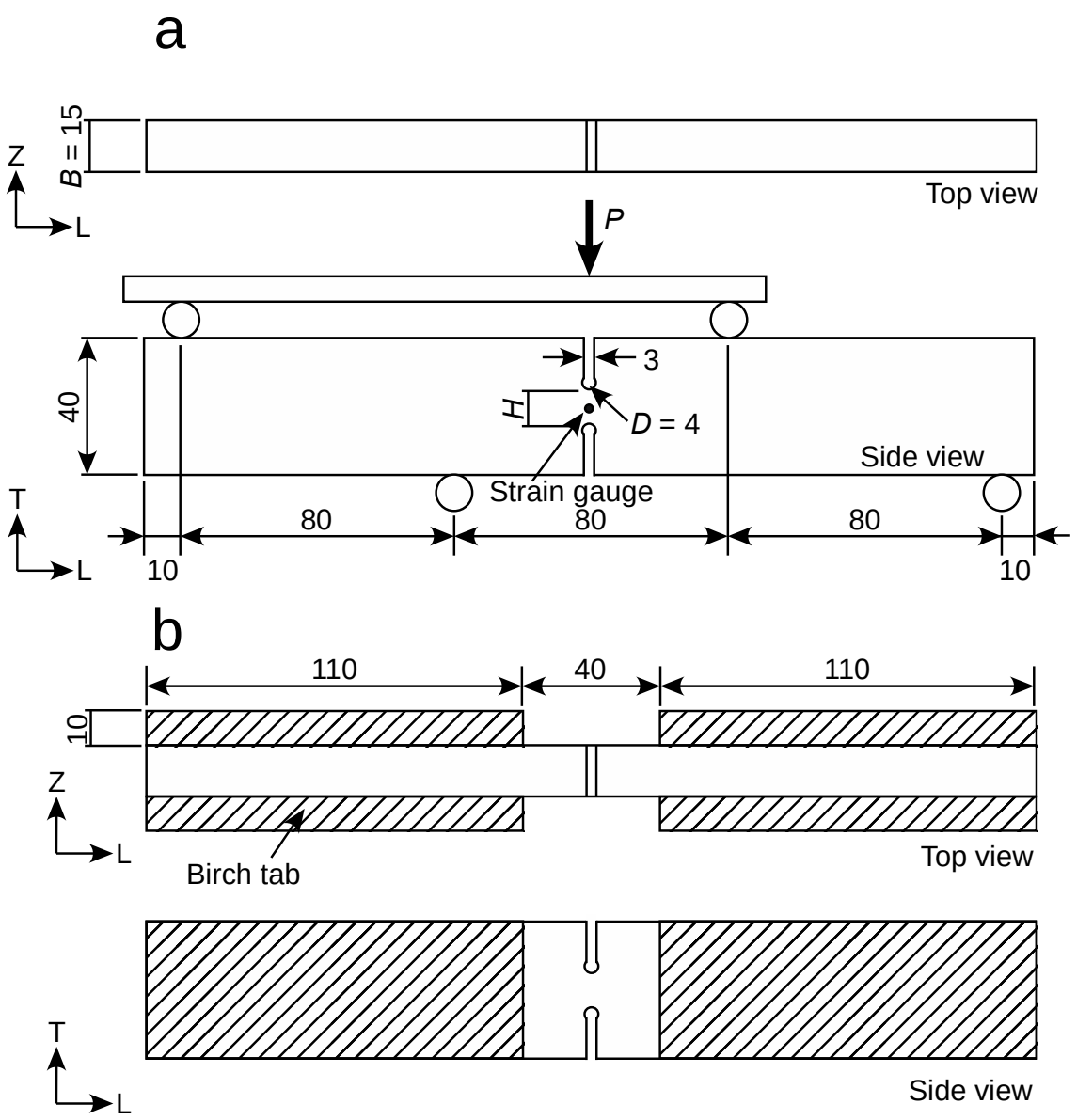

Fig. 1 (a) Tab-free specimen and diagram of the asymmetric four-point loading and (b) tabbed specimen. Units: mm. L and T represent the length and width directions of the MDF sheet, respectively.

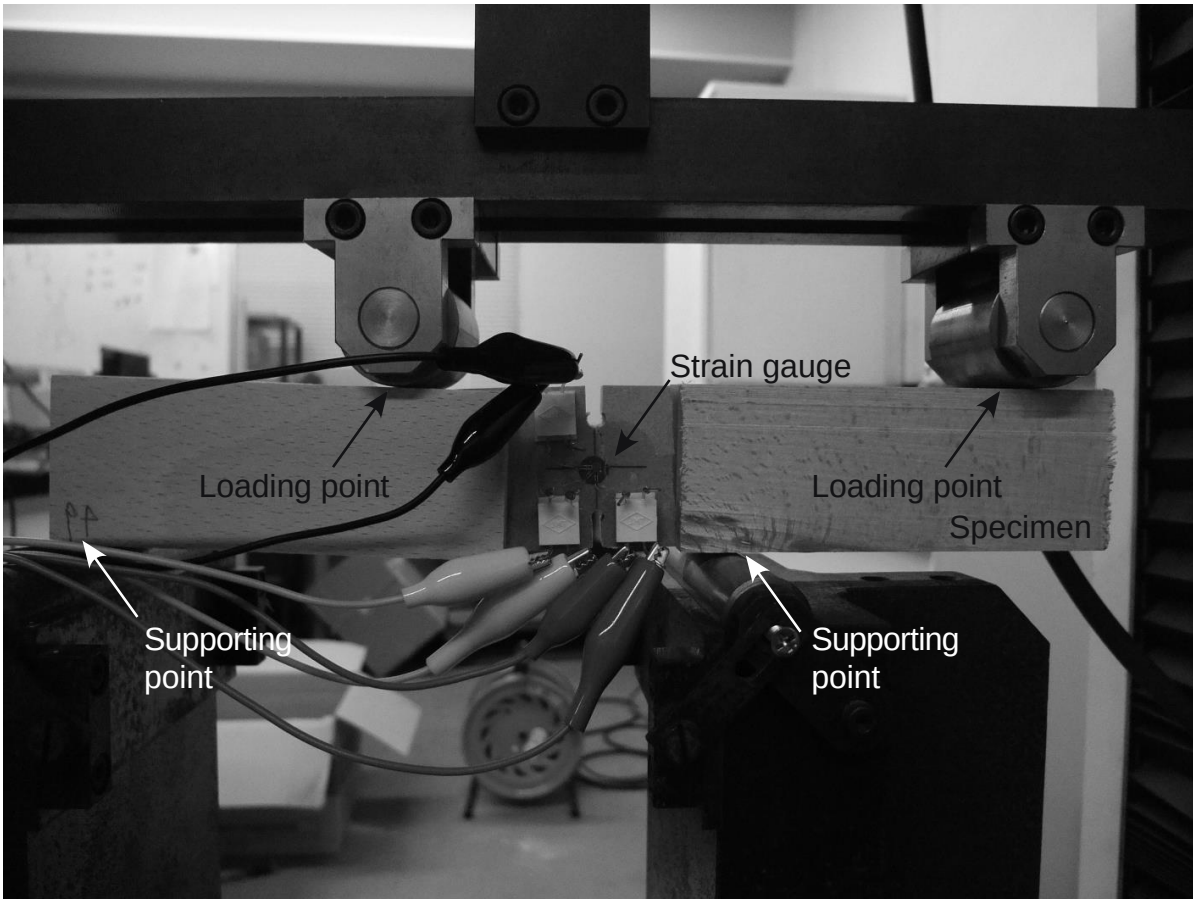

Fig. 2 Asymmetric four-point bending (AFPB) test setup.

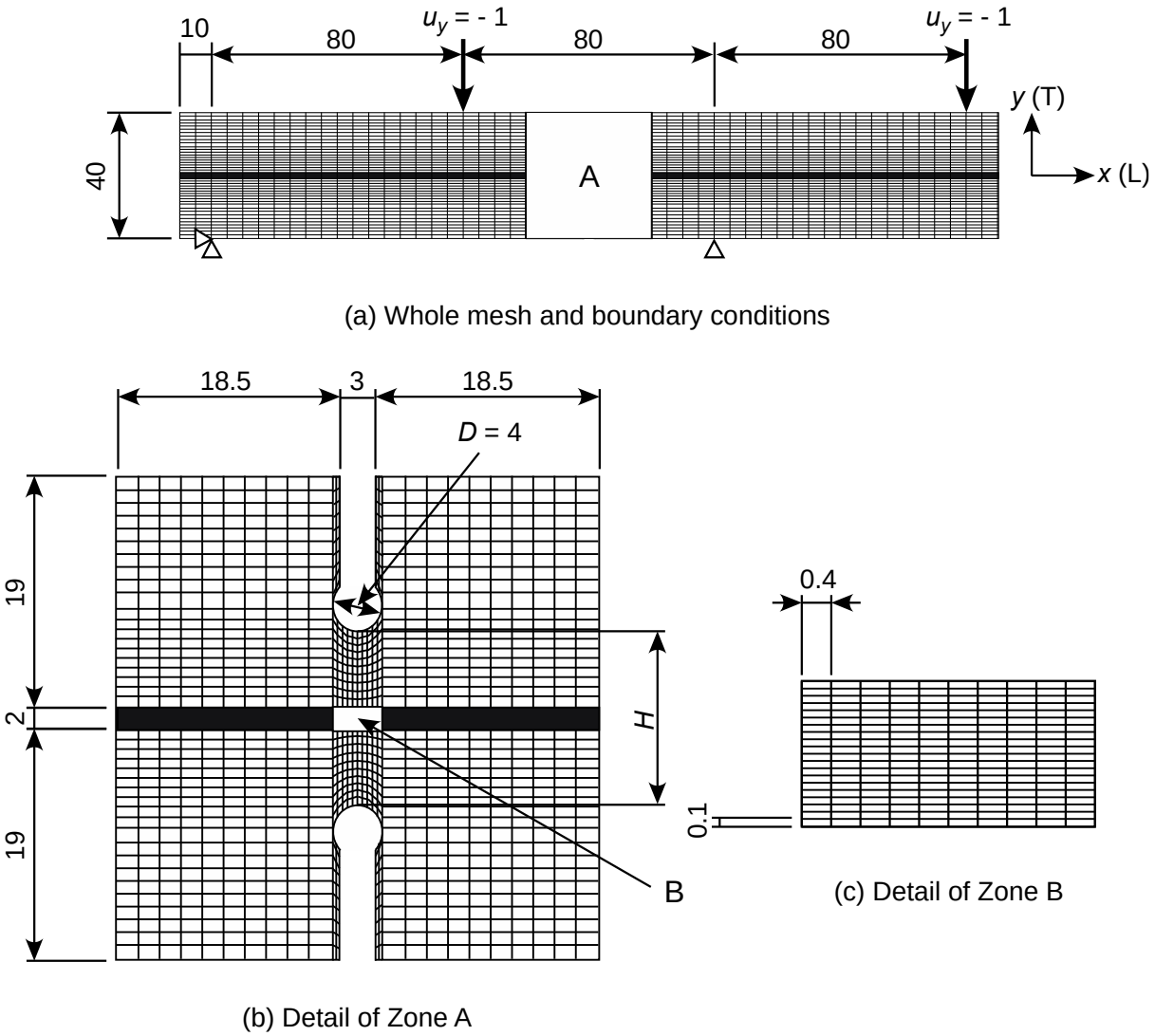

Fig. 3 Finite element model for the AFPB test. (a) Overall mesh, (b) detail of zone A, and (c) detail of zone B. Unit = mm.

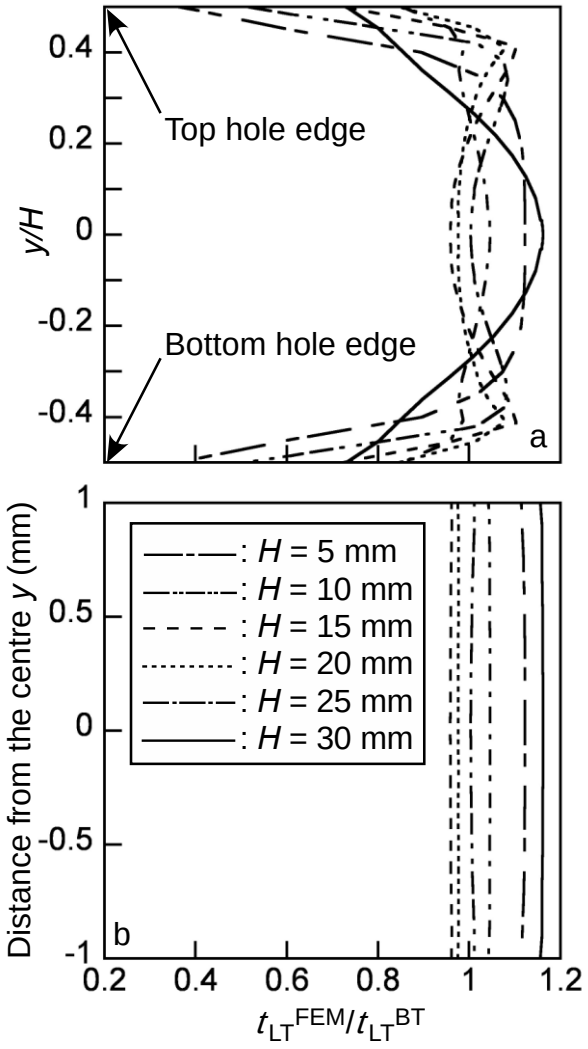

Fig. 4 Distributions of the $\tau_{LT}^{FEM}/\ \tau_{LT}^{BT}$ values between the notch roots (a) and around the gauge region (b) obtained from the 2D FEAs.

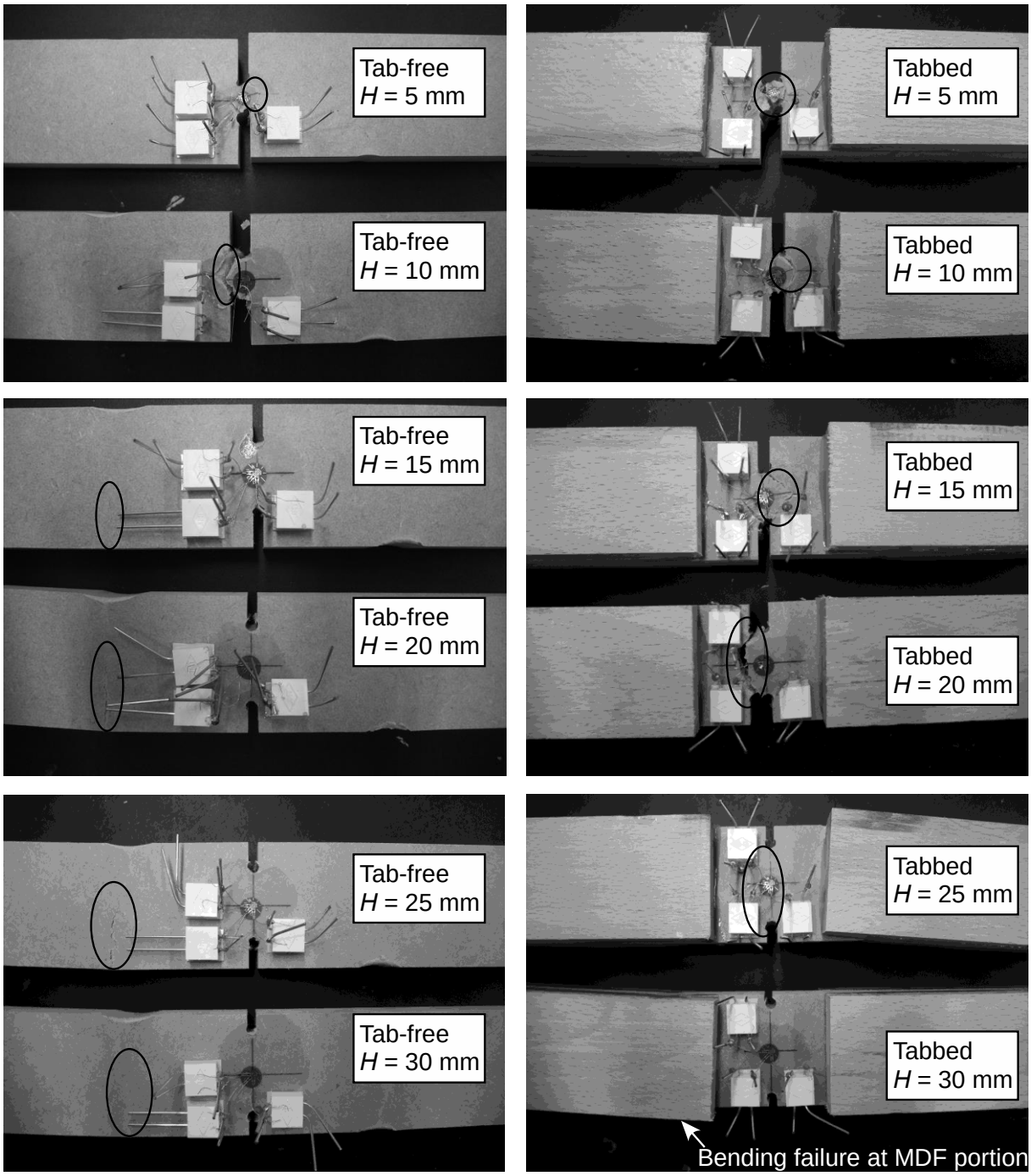

Fig. 5 Typical failure patterns corresponding to the distance between the notch roots *H*. Failure is indicated in the ellipsoid except for the tabbed specimen with *H* = 30 mm.

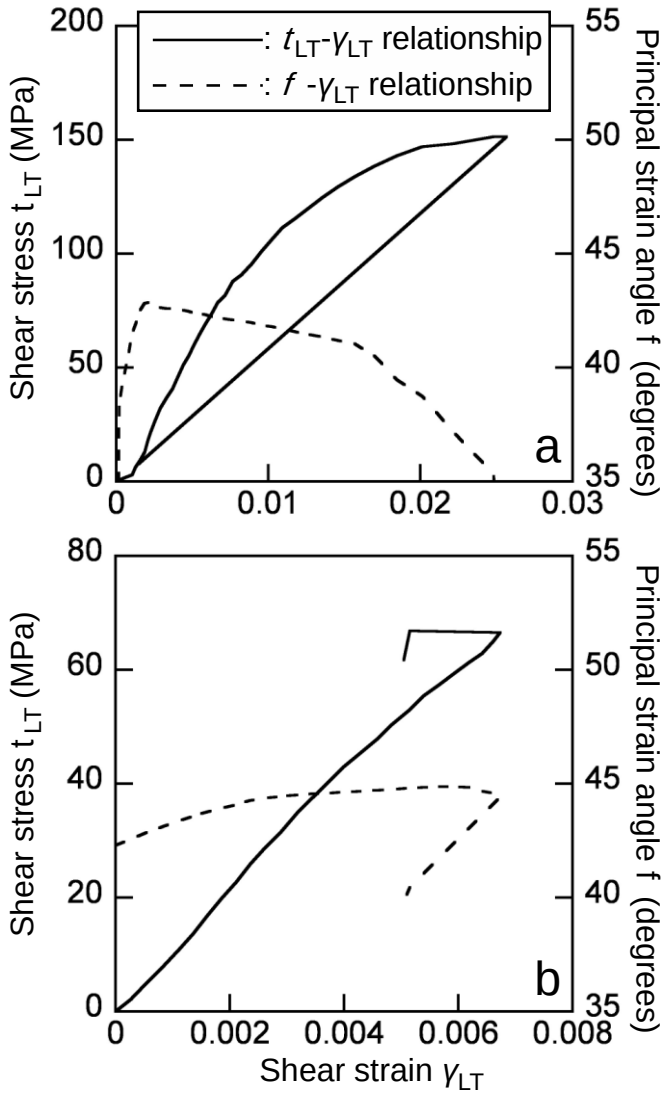

Fig. 6 Typical examples of the shear stress/shear strain relation and the principal strain angle/shear strain relation. (a): Tabbed specimen with H = 15 mm, failure by shearing force at the gauge portion and (b): Tabbed specimen with H = 30 mm, failure by bending moment at the point behind the inner loading point.

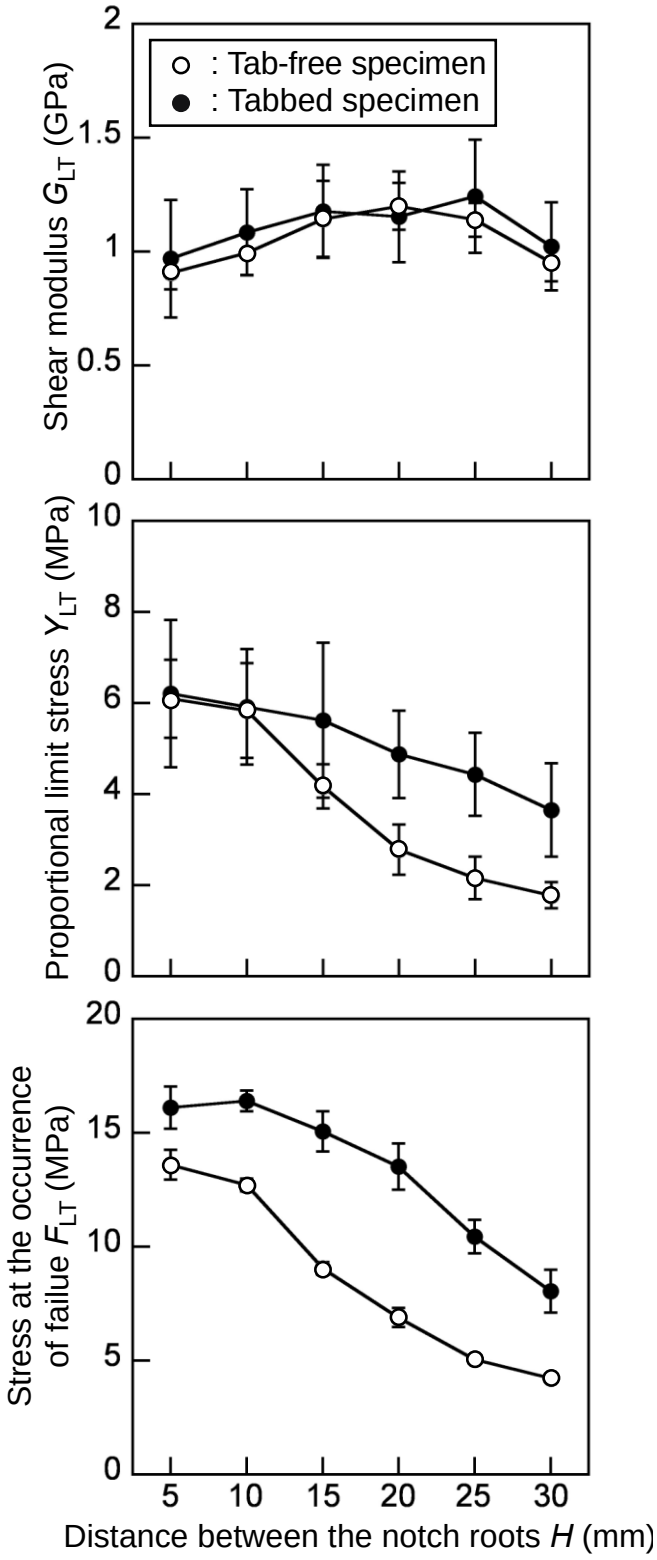

Fig. 7 Shear modulus G_{LT}, proportional limit stress Y_{LT}, and stress at the occurrence of failure F_{LT} corresponding to the distance between the notch roots H. Results are average ± SD.